RESEARCH PAPER

On-chip manipulation and trapping of microorganisms using a patterned magnetic pathway

R. Venu · B. Lim · X. H. Hu · I. Jeong ·
T. S. Ramulu · C. G. Kim

Abstract We demonstrate on-chip manipulation and trapping of individual microorganisms at designated positions on a silicon surface within a microfluidic channel. Superparamagnetic beads acted as microorganism carriers. Cyanobacterium *Synechocystis* sp. PCC 6803 microorganisms were immobilized on amine-functionalized magnetic beads (Dynabead® M-270 Amine) by 1-ethyl-3-(3-dimethylaminopropyl)carbodiimide (EDC)–*N*-hydroxysulfosuccinimide coupling chemistry. The magnetic pathway was patterned lithographically such that half-disk $Ni_{80}Fe_{20}$ (permalloy) 5 μm elements were arranged sequentially for a length of 400 micrometers. An external rotating magnetic field of 10 mT was used to drive a translational force (maximum 70 pN) on the magnetic bead carriers proportional to the product of the field strength and its gradient along the patterned edge. Individual microorganisms immobilized on the magnetic beads (transporting objects) were directionally manipulated using a magnetic rail track, which was able to manipulate particles as a result of asymmetric forces from the curved and flat edges of the pattern on the disk. Transporting objects were then successfully trapped in a magnetic trapping station pathway. The transporting object moves two half-disk lengths in one field rotation, resulting in movement at $\sim$24 μm s^{-1} for 1 Hz rotational frequency with 5 μm pattern elements spaced with a 1 μm gap between elements.

1 Introduction

The ability to analyze the cellular contents of individual microorganisms would significantly benefit our understanding of many mechanisms in the minute world of microorganism biology (Pawel et al. 2011). Several technologies are currently available for direct intrinsic studies leading to single cell analysis, including capillary electrophoresis and flow cytometry (Krylov and Dovichi 2000). Recent, rapid developments in lab-on-a-chip technology offer significant advantages over standard techniques for the analysis of individual microorganisms. Integrating the trapping concept to current available technologies will provide the opportunity to analyze microorganisms at the micro levels.

Different kinds of techniques have been developed to trap the individual cells such as optical, hydrodynamic, dielectrophoretic, and acoustic traps (Lindstrom et al. 2010). However, these techniques have some limitations, e.g., (1) optical tweezers could eventually damage the cell structure; (2) hydrodynamic trapping is not suitable for long-term analysis; (3) dielectrophoretic trapping requires instead the use of non-conductive bacterial growth medium; and (4) acoustic trapping does not have long-term cell viability (Lindstrom et al. 2010).

R. Venu · B. Lim · X. H. Hu · I. Jeong ·
T. S. Ramulu · C. G. Kim (✉)
Center for NanoBioEngineering & SpinTronics (nBEST),
Chungnam National University, Daejeon, 305-764, South Korea
e-mail: cgkim@cnu.ac.kr

R. Venu · B. Lim · X. H. Hu · I. Jeong ·
T. S. Ramulu · C. G. Kim
Department of Materials Science and Engineering,
Chungnam National University, Daejeon 305-764, South Korea

In this context, the magnetic beads bind to the cells (transporting object), then guide these transporting objects under magnetic fields that are receiving a great interest in manipulation, and trapping the individual microorganisms at designated positions on the solid surfaces. An advantage of this system is that cell loading on the magnetic beads cannot impact the cell viability and cell structure (Ito et al. 2005). In addition, the magnetic fields do not screen by biologic content and bacterial growth medium.

Magnetic beads with functionalized surfaces are widely used as carriers for manipulation, separation, and biomolecular sensing (Brzeska et al. 2004; Gijs 2004; Karle et al. 2010; Karle et al. 2011; Safarik and Safarikova 2004). In the past few years, many approaches have been developed for the on-chip manipulation and transport of functionalized magnetic beads using micro-fabricated current-carrying wires and coils (Deng et al. 2001; Ramadan et al. 2006; Wirix-Speetjens et al. 2005). However, these devices generate heat on the chip that could damage biologic entities. In addition, these devices do not allow for the manipulation of beads over distances of few tens of micrometers.

The use of soft magnetic microstructures is the best means by which to overcome these drawbacks to the on-chip manipulation and transport of biomagnetic carriers. Traditionally, on-chip soft magnetic microstructures are fabricated by $Ni_{80}Fe_{20}$ (permalloy) material because it shows maximal magnetic permeability (μ_m) and a low coercive field (Hc) under weak magnetic fields (Liu et al. 2009). Gunnarsson et al. (2005), Smistrup et al. (2006), and Anandakumar et al. (2009) have used permalloy soft magnetic microstructures to translocate magnetic beads. Their studies focused on precisely controlling the translocation of magnetic beads through forward and backward motion by varying the designs of soft magnetic microstructures. These studies emphasize that the design and fabrication of new microstructures is useful in the development of novel biologic devices for manipulating individual microorganisms.

Herein, we demonstrate the manipulation and trapping of individual microorganisms at designated positions on a silicon substrate within a microfludic channel. We chose the photosynthetic algae Synechocystis sp. PCC 6803 as a sample microorganism to translocate with magnetic bead carriers. Synechocystis is a model organism for the study of the mechanisms of photosynthesis, plant plastid evolution, and plant adaptation to environmental stressors (Anderson and Mcintosh 1991). Cyanobacterium Synechocystis sp. PCC 6803 cells were immobilized on amine-functionalized magnetic beads (Dynabead® M-270 Amine) using 1-ethyl-3-(3-dimethylaminopropyl)carbodiimide (EDC)–N-hydroxysulfosuccinimide (NHS) coupling chemistry. The Synechocystis sp. PCC 6803 cells immobilized on the magnetic beads (transporting

objects) were directionally manipulated on a magnetic rail track and successfully trapped in a magnetic trapping station.

2 Experimental procedures

2.1 Materials

Amine-functionalized superparamagnetic beads (Dynabead® M-270 Amine) 2.8 μm in diameter were procured from Life Technologies (Carlsbad, CA, USA). Silicon wafers coated with 200 nm SiO_2 were obtained from Wafermart Co. (Seoul, Korea). Photoresist (AZ 5214-E) and the corresponding developer were purchased from AZ Electronic Materials (Branchburg, NJ, USA). SU-8 50 was purchased from Microchem (Newton, MA). Poly(dimethylsiloxane) (Sylgard 184) was procured from Dowhitech Silicon Co., Ltd (Seoul, Korea). We used high performance liquid chromatography water from Sigma–Aldrich (St Louis, MO, USA) for photolithography experiments. EDC and NHS were purchased from Sigma–Aldrich (USA). All chemicals used for cell media were obtained from Sigma–Aldrich. We used ultrapure water for all cell experiments and in all media.

2.2 Methods

2.2.1 Cell culture

Wild-type photosynthetic algae Synechocystis sp. strain PCC 6803 was cultured in BG-11 medium at 30 °C. Cultures were harvested up to a density of $\sim 10^6$ cells mL^{-1}. We concentrated these cultures to $\sim 10^8$ cells mL^{-1} by centrifugation for 2 min at 900 rpm.

2.2.2 Loading Synechocystis sp. PCC 6803 cells onto magnetic beads

A 1 mL aliquot of Synechocystis sp. PCC 6803 cell suspension was centrifuged in an Eppendorf tube, and the supernatant was discarded. The cells were resuspended in PBS buffer (1 mL, pH 7.4) and concentrated by centrifugation; this step was repeated three times for washing. The washed cells were mixed with 50 μL EDC (100 mM) dissolved in PBS buffer (pH 5.8). The tube was placed on a vortex shaker and gently agitated for 15 min at 27 °C, followed by three washes in PBS buffer (1 mL, pH 5.8). The EDC-modified Synechocystis sp. PCC 6803 cells were resuspended in PBS buffer (pH 7.4) containing 50 μL NHS (100 mM). The tube containing cells was again placed on a vortex shaker, gently agitated for 15 min at 27 °C, and washed three times with PBS buffer (1 mL, pH 7.4). The

NHS-modified *Synechocystis* sp. PCC 6803 cells were treated with 10 μL of PBS buffer (pH 7.4) containing 2.8-μm-sized amine-functionalized magnetic beads (approx. 30 mg mL^{-1}) and gently agitated for 15 min at 27 °C. *Synechocystis* sp. PCC 6803 cells loaded with magnetic beads were isolated with an external magnetic field followed by three washes with PBS buffer (pH 7.4). The isolated solution was made up to 0.5 mL using BG-11 cell media.

2.2.3 Fabrication of a magnetic permalloy pattern for the rail track and trapping station

A 5-μm-sized half-disk permalloy pattern of 400 micrometers length was drawn by means of AutoCAD® software (version 2010, Autodesk, Inc., San Rafael, CA, USA), and a chromium metal photomask of the pattern was prepared by electron beam lithography. An inverse image of the pattern was created in positive photoresist on top of the silicon wafer substrate using a chromium metal photomask and exposure to ultraviolet light with a mask aligner.

The pattern was stenciled on the photoresist layer by first rinsing the silicon wafer substrate in developer and rinsing again in deionized water. A 100-nm-thick layer of permalloy film was sputtered on the stenciled pattern by means of a direct current magnetron sputtering system. The photoresist was removed by a lift-off process, leaving the desired structure of the half-disk permalloy pattern on the silicon wafer substrate.

2.2.4 Monitoring setup for transporting objects

A schematic drawing of the magneto-microfluidic chip for the manipulation and trapping of individual microorganisms is shown in Fig. 1. The *Synechocystis* sp. PCC 6803 cells loaded with magnetic beads were translocated along the pathway elements in a microfluidic channel. We fabricated the microfluidic channel on the magnetic-patterned silicon substrate by means of a previously reported procedure (Duffy et al. 1998). Briefly, photolithography was used to fabricate features in SU-8 photoresist (SU-8 50) on silicon wafers, Polydimethylsiloxane (PDMS) was poured on the master and cured thermally (75 °C), and the resulting layer of PDMS contained the microfluidic channel. The magneto-microfludic chip was fabricated by oxidizing both the silicon substrate with the half-disk permalloy pathway and the layer of PDMS containing the channel in oxygen plasma. The chip was then sealed by properly aligning the surfaces into contact. The magneto-microfludic chip was transferred into a preheated oven kept at 75 °C for 45 min. A system for injecting a diluted solution of *Synechocystis* sp. PCC 6803 cells loaded with magnetic beads into the microfluidic channel was prepared
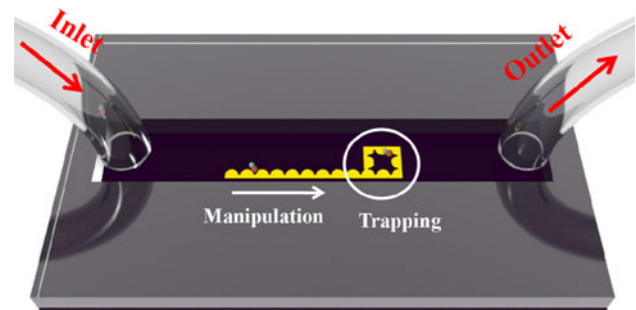

Fig. 1 Schematic drawing of the magneto-microfluidic chip used for the manipulation and trapping of microorganisms

using tubing attached to the inlet and outlet of the magnetic-patterned microfluidic chip. The motion of the transporting objects along the pathway was observed with an optical microscope connected to a computer.

### 2.2.5 Driving force for transporting objects

The driving force for the translocation of objects was produced by a rotational magnetic field. The rotating magnetic field was produced by ferrite core solenoids arranged along mutually orthogonal axes (*x*- and *y*-axes). Two current sources were controlled by LabVIEW software (version 7.1, National Instruments, Austin, TX, USA) to supply sinusoidal waveforms to each solenoid coil. The current sources along the orthogonal axes were adjusted with a 90° phase difference described by $\vec{H}_x = H_0 \cos(\omega t)\,\hat{i}$ and $\vec{H}_y = H_0 \sin(\omega t)\,\hat{j}$ to generate a rotating magnetic field in the *x*–*y* plane (Anandakumar et al. 2010). An external rotating field H_0 of 10 mT was obtained by applying a 0.54 A current to each ferrite core solenoid in order to induce a driving force on the magnetic bead carriers.

3 Results and discussion

3.1 Characterization of the transporting objects

The carrier (amine-functionalized magnetic beads) loaded with *Synechocystis* sp. PCC 6803 cells was prepared by EDC–NHS coupling chemistry (Fig. 2). The carboxylic groups present on the *Synechocystis* sp. PCC 6803 cell wall were activated with EDC. The EDC-modified *Synechocystis* sp. PCC 6803 cells were subjected to NHS to produce amine-reactive NHS esters. The NHS-modified *Synechocystis* sp. PCC 6803 cells were treated with amine-functionalized magnetic beads to produce covalent amide bonds between the *Synechocystis* sp. PCC 6803 cells and the magnetic beads.

Fig. 2 EDC–NHS coupling chemistry used to immobilize microorganisms on magnetic beads
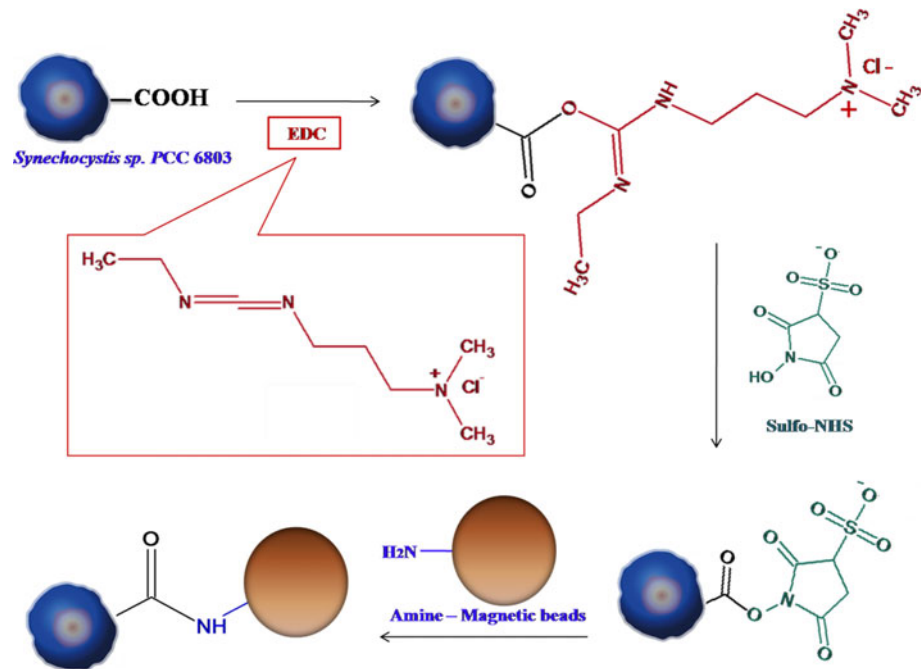
Confocal microscopy was used to characterize the immobilization of *Synechocystis* sp. PCC 6803 cells on the magnetic beads. Bright field images of the *Synechocystis* sp. PCC 6803 cells, magnetic beads, and *Synechocystis* sp. PCC 6803 cells coupled to the magnetic beads are shown in Fig. 3a–c, respectively. The inset in Fig. 3c shows a high-resolution bright field image of a single *Synechocystis* sp. PCC 6803 cell attached to a single magnetic bead. It shows the clear differentiation between the cells and the magnetic beads. Fig. 3c shows images confirming the immobilization of *Synechocystis* sp. PCC 6803 cells on the magnetic beads. The algae *Synechocystis* sp. PCC 6803 contains chlorophyll pigment, which fluoresces at wavelengths of 620–630 nm (Schubert et al. 1989). Thus, fluorescence images were also used to confirm the immobilization of *Synechocystis* sp. PCC 6803 cells on the magnetic beads. The fluorescence image obtained from the field of view of Fig. 3c is shown in Fig. 3e. Figure 3f was obtained by combining the fluorescence (Fig. 3e) and bright field images (Fig. 3c) of the transporting objects. As shown in Fig. 3f, the *Synechocystis* sp. PCC 6803 cells coupled to the magnetic beads fluoresced, indicating that the *Synechocystis* sp. PCC 6803 cells were immobilized on the magnetic beads. These results also suggest that the cells coupled to the magnetic beads in a one-to-one ratio (~ 95 %).

3.2 Driving forces for directional control of the transporting objects

Directional control of transporting objects can be accomplished by asymmetric forces for forward and backward movements. These asymmetric forces are induced by the asymmetry of curved and flat edges of half-disk elements. The magnetic field is difficult to measure for micro-scale elements under certain applied fields due to the size limitation of measuring sensors in magnetometers, but it can be obtained by the finite element method (FEM) simulation by means of 3D Maxwell software (Sinha et al. 2012). For simulation, it is required to input the initial M-H curve of the materials. It was measured from the Vibrating Sample Magnetometer (VSM) (see Supplementary information Fig.S1). The saturation magnetization of the permalloy thin film is ~ 668 emu cc^{-1}.

Figure 4a shows the change of magnetic flux distribution around half-disk patterns for the different configurations of the rotating of the magnetic field. When the direction of the magnetic field is angle 0° from the pathway axis, then the magnetic flux density is to be higher between the two corners. However, after changing the field direction to angle 45°, the density of magnetic flux can shift to the field direction, which means that the magnetic bead can move from the corner of angle 0° to the position of angle 45°, following the high density point of magnetic flux.

Calculation of the magnetic forces along the curved and flat edges of a half disk requires 2 coordinates: polar coordinates (ρ, φ) for the curved edge and rectangular coordinates (x, y) for the flat edge (Fig. 4b). The driving forces of the magnetic beads along the pattern are given as a function of the magnetic field and its gradients in each coordinate as explained by the following equations in terms of magnetic field intensity B (Varadan 2008):
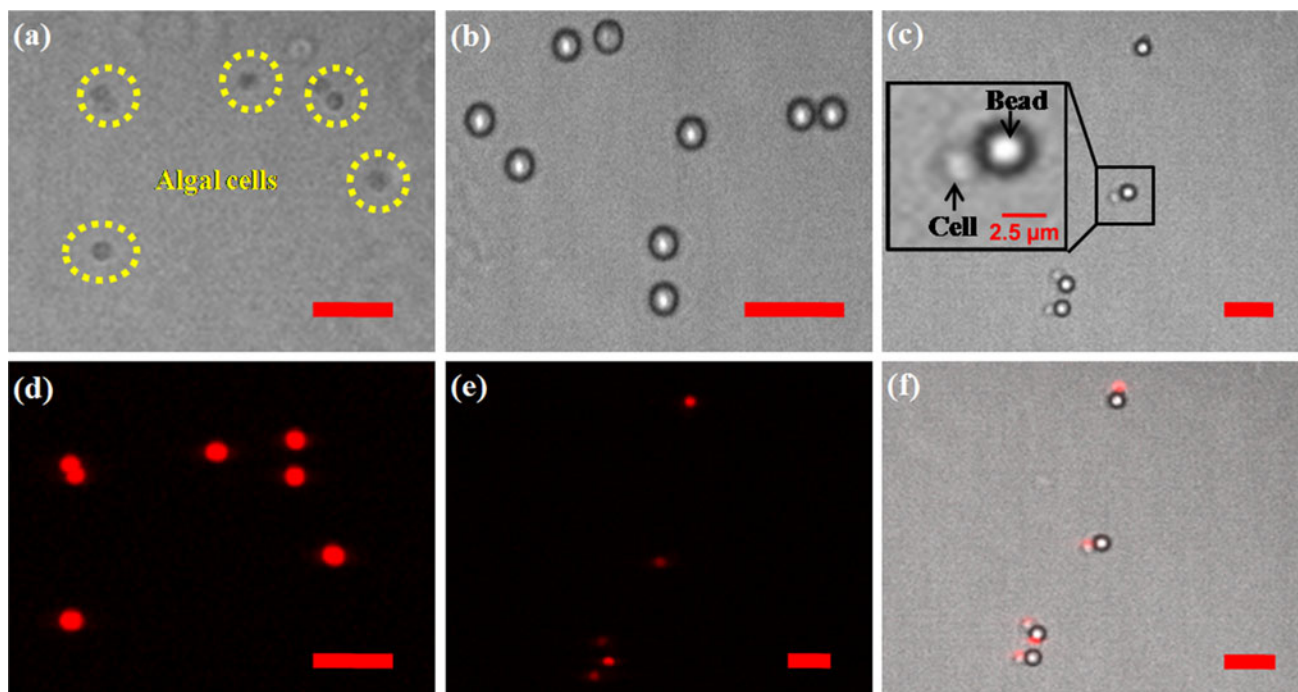
Fig. 3 Bright field images of **a** *Synechocystis* sp. PCC 6803 cells, **b** magnetic beads, and **c** *Synechocystis* sp. PCC 6803 cells immobilized on magnetic beads (transporting objects). Fluorescence images of **d** *Synechocystis* sp. PCC 6803 cells and **e** *Synechocystis* sp. PCC 6803 cells immobilized on the magnetic beads (transporting objects). **f** Image was obtained by overlapping images (**c**) and (**e**). The *inset* **c** represents a high-resolution bright field image of a single cell immobilized on a single magnetic bead. *Red lines* represent *scale bars* of 10 μm

$$\overrightarrow{F} = \frac{\chi_V V}{2\mu_o} \nabla(\overrightarrow{B} \cdot \overrightarrow{B})$$

$$= F_\rho \hat{e}_\rho + F_\varphi \hat{e}_\varphi \quad \text{Polar coordinates} \tag{1a}$$

$$F_\rho = \frac{\chi_V V}{\mu_o}\left(B_\rho \frac{\partial B_\rho}{\partial \rho} + B_\varphi \frac{\partial B_\varphi}{\partial \rho}\right),$$

$$F_\varphi = \frac{\chi_V V}{\mu_o}\frac{1}{\rho}\left(B_\rho \frac{\partial B_\rho}{\partial \varphi} + B_\varphi \frac{\partial B_\varphi}{\partial \varphi}\right)$$

$$\overrightarrow{F} = F_x \hat{e}_x + F_y \hat{e}_y \quad \text{Rectangular coordinates} \tag{1b}$$

$$F_x = \frac{\chi_V V}{\mu_o}\left(B_x \frac{\partial B_x}{\partial x} + B_y \frac{\partial B_y}{\partial x}\right),$$

$$F_y = \frac{\chi_V V}{\mu_o}\left(B_x \frac{\partial B_x}{\partial y} + B_y \frac{\partial B_y}{\partial y}\right)$$

Here, V is the volume of the bead (m³), χ_V is the magnetic volume susceptibility (SI) of the bead, μ_0 is the permeability of vacuum ($4\pi \times 10^{-7}$ N A^{-1}), and B is the magnetic flux distribution around the half-disk patterns (T). B_ρ, B_φ and B_x, B_y are the components of the magnetic field intensity (mT) in polar (ρ, φ) and rectangular (x,y) coordinates, respectively. F_ρ, F_φ and F_x, F_y are the components of the magnetic force in polar and rectangular coordinates, respectively. The force components can be calculated by the local distribution of the magnetic fields.

Here, it is noted that rotational force F_φ and vertical force F_y correspond to the driving force for the carrier bead, whereas radial force F_ρ and horizontal force F_x govern the distance between the pattern and bead.

The force components at the points with a distance of ~ 1.4 μm from the half-disk edge, equal to the bead radius, were numerically calculated by Eqs. 1(a) and 1(b) based on the local distribution of the magnetic field along the edge of the half disk under an applied field of 10 mT. As shown in Fig. 4c, the rotational force F_φ at the curved edge has a maximum of about ~ 70 pN at an angle between field and bead, $\varphi = \pi/4$; positive forces in the range of $\sim -30°$ to $\sim 0°$ increase the bead position angle φ to approach 0°, but negative forces in the range of $\sim 0°$ to $\sim 30°$ decrease the angle φ to approach 0°. Eventually, the bead shifts to the 0° position, i.e., the field direction. However, the vertical force F_y along the mid region of the flat edge is nearly 0 pN, indicating that the rotational force at the curved edge is larger than the force at the flat edge.

Radial force F_ρ is negative (attractive) for an angle range of $\sim -45°$ to $\sim 45°$ and positive (repulsive) for an angle range of both $\sim 50°$ to $\sim 85°$ and $\sim -50°$ to $\sim -85°$. If radial force F_ρ is negative irrespective of ρ, then the bead will approach the pattern center. In fact, F_ρ is a function of ρ and becomes positive for $\rho \sim 6.0$ μm at an
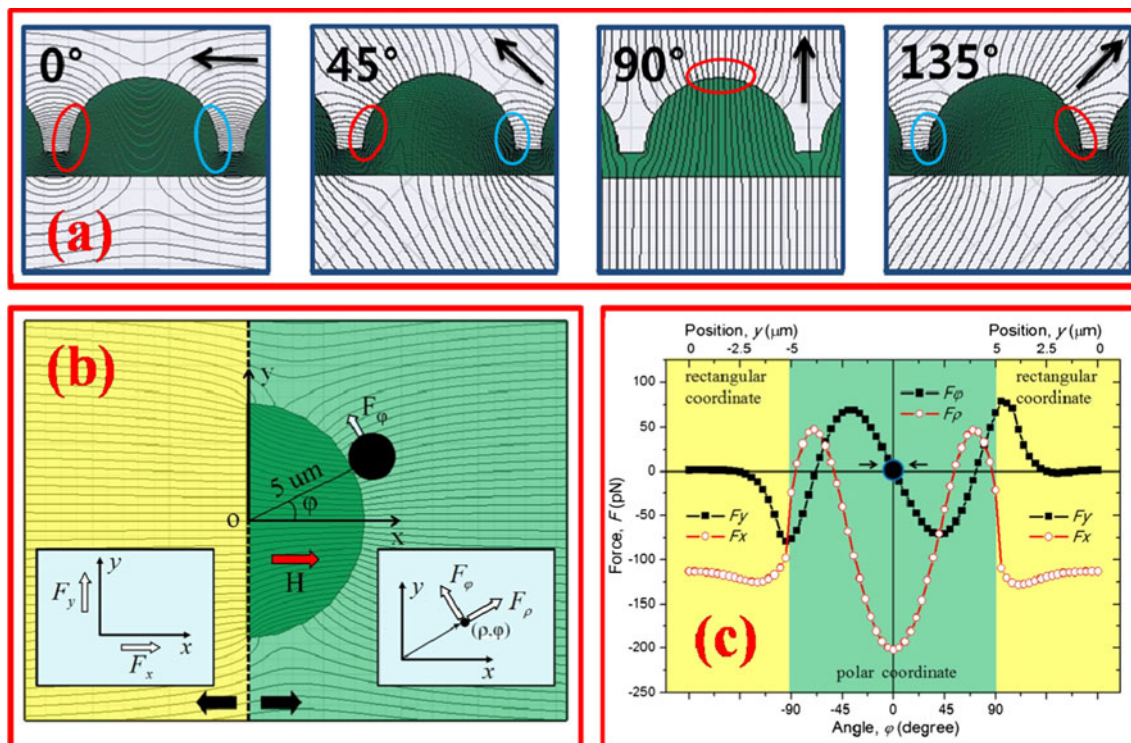
Fig. 4 a The induced field counter around a half-disk pathway under an applied magnetic field from 0° to 135°. **b** The induced field contour around a half disk of permalloy under an applied magnetic field and **c** the rotational and radial force on a magnetic bead with a diameter of 2.8 μm around a half disk of permalloy under an applied field of 10 mT. The *insets* in b: schematic representation of rectangular coordinates (*left side*) and polar coordinates (*right side*)

angle $\varphi = 0°$, indicating that the bead is positioned at ∼0.4 μm inside the pattern edge.

When the driving forces F_{φ} and F_y overcome the retarding forces—which are the viscous force, the sticking force, the drag force, etc., (Elizabeth and Geoffery 2012, Johansson et al. 2010)—the bead is capable of motion. The retarding force is increased with the speed of the bead. When the rotating field frequency is lower than the critical frequency related with the retarding force, then a bead rotates along the pattern edge revealing harmonic rotation with the field. The critical frequency is a function of the pattern and bead sizes as well as the external field strength (Hu et al. 2012). The critical frequency for 5 μm elements' pattern was measured to be 1 Hz for 10 mT field strength.

The moving direction of beads along the curved edge of the half-disk permalloy pathway can be controlled by a directional rotating magnetic field because the rotational force along the curved edge of the next adjacent element is larger than that of the force along the flat edge. As a result, the transporting object can be manipulated in the forward or backward directions by changing the rotational direction of the external magnetic field.

3.3 Manipulation of microorganisms

Directional manipulation of microorganisms was demonstrated by transporting objects on the sequential half-disk magnetic pattern. Figures 5a–i show the curved edge of the permalloy half-disk pathway for directional control with respect to the direction of the external rotating magnetic field. The forward motion of the transporting object on the curved edge is attributed to the clockwise rotation of the external magnetic field, which is shown in Fig. 5a–e. Backward motion of the transporting object was achieved by reversing the rotating magnetic field in a counterclockwise direction, which is shown in Fig. 5f–i. The forward and backward motions of microorganisms (directional manipulation) were also confirmed by fluorescence images (see Supplementary Information Fig. S2). In our experiments, the transporting object moves two half-disk lengths in one field rotation, resulting in movement at ∼24 μm s^{-1} for 1 Hz rotational frequency with 5 μm pattern elements spaced with a 1 μm gap between elements. Comparing the manipulation movement of microorganisms with other methods, the present method shows a slightly lower manipulation movement of microorganisms; consider hunt et al., (2008) manipulation of the

Fig. 5 **a–e** Images of the forward motion of a transporting object on the curving edge of the half-disk permalloy pattern with respect to a clockwise-rotating magnetic field. **f–i** Images of the backward motion of a transporting object on the curving edge of the half-disk permalloy pattern with respect to a counterclockwise-rotating magnetic field (See Supplementary Information Video 1). *Dark purple lines* represent *scale bars* of 10 µm
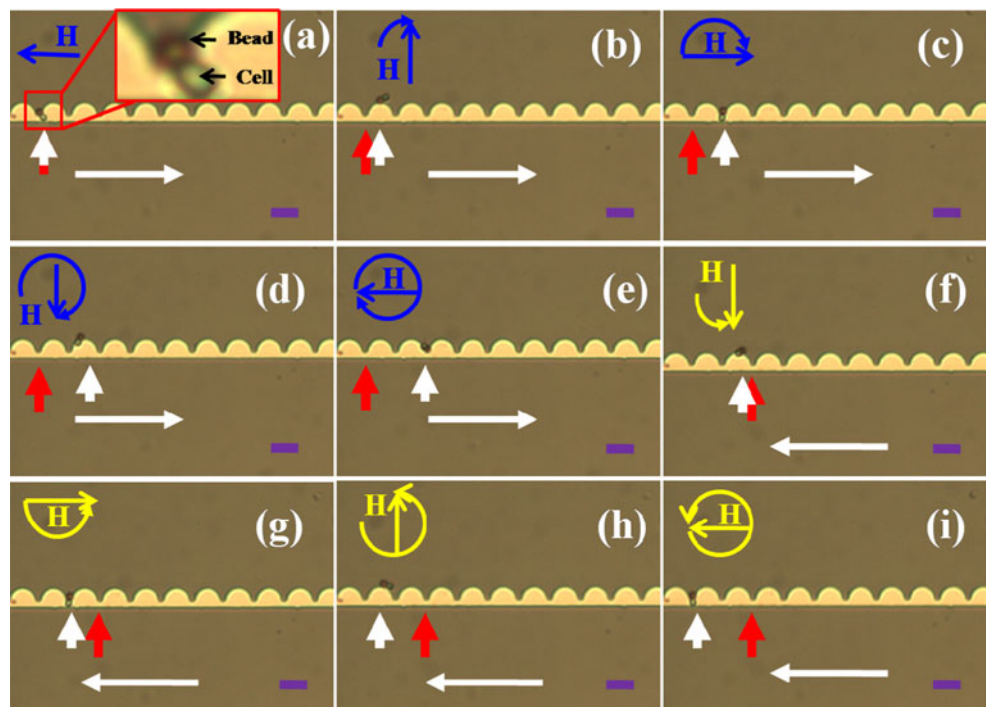

Fig. 6 **a–g** Images of the trapping of a transporting object in a magnetic trapping station using the curving edges of the half-disk permalloy pattern by applying a rotating magnetic field in the clockwise direction. **h–i** Images of the transporting object motion within the magnetic trapping station using the curving edges of the half-disk permalloy pattern by applying a rotating magnetic field in the counterclockwise direction (See Supplementary Information Video 2). *Red lines* represent *scale bars* of 10 µm
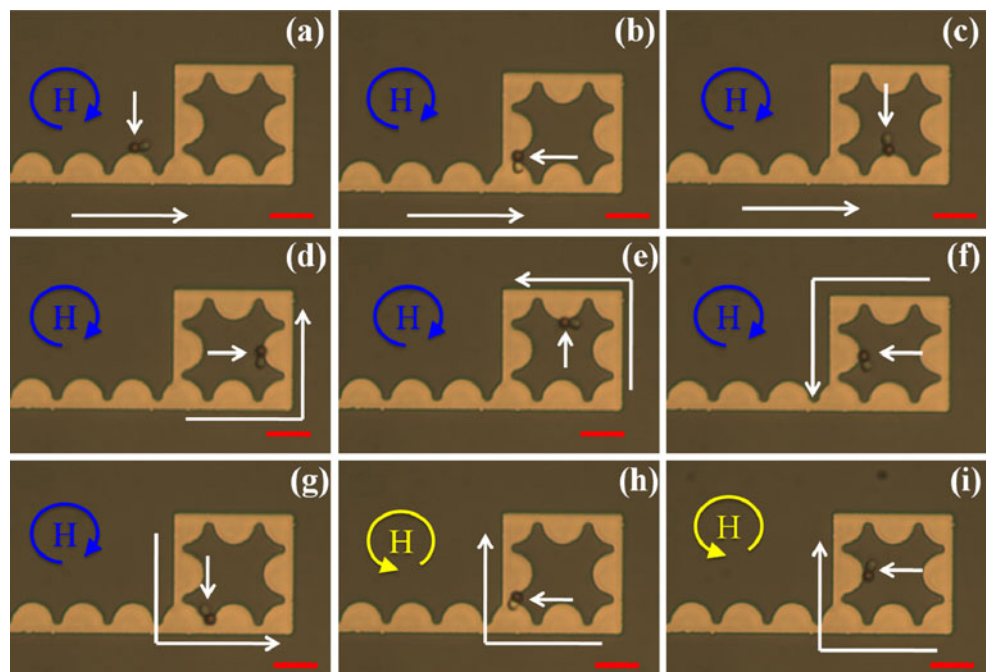
microorganisms (yeast cells) with movement of 30 µm s^{-1} by the dielectrophoretic technique. However, the present method has the capability to increase the manipulation movement of microorganisms by increasing the critical frequency, while the increasing of the critical frequency occurs by the increasing of rotational field strength.

3.4 Trapping of microorganisms

We used the described technology to trap microorganisms at designated positions, thereby developing a magnetic trapping station for individual microorganisms. First, we carried out an experiment to tarp a magnetic bead in the

magnetic trapping station by the external rotating magnetic field (see Supplementary Information Fig. S3). Later, the bead attached to the *Synechocystis* sp. PCC 6803 (transporting object) was trapped in a magnetic trapping station at a designated position. The transporting object enters into the magnetic trapping station through continuous application of an external clockwise-rotating magnetic field. The transporting object moves around the magnetic trapping station as shown in Fig. 6a–g. As shown in Fig. 6h–i, the transporting object in the magnetic trapping station is not capable of escaping from the magnetic trapping station even after the external rotating magnetic field is changed to rotate in a counterclockwise direction, confirming that the individual microorganism was successfully trapped in a magnetic trapping station. Trapping of microorganisms in a magnetic trapping station was also confirmed by the fluorescence images (see Supplementary Information Fig. S4). This novel approach is capable of trapping the single microorganism in a magnetic trapping station pathway. The single microorganism trap was achieved by the following phenomenon. The two transporting objects were moving on the magnetic rail track toward a magnetic trapping station with a little distance of ~ 5 μm; the first moving transporting object was entered into the magnetic trapping station by continuously applying an external rotating magnetic field. After entering the first transporting object into the magnetic trapping station, we immediately changed the direction of the external rotating magnetic field; as a result, the second transporting object moves away from the magnetic trapping station. Thus, this manipulation and trapping technique can be applied to the analysis of the content of individual microorganisms by integrating the technique with lab-on-a-chip systems.

4 Conclusions

We have demonstrated a novel magnetic method to manipulate and trap microorganisms at designated positions on a silicon surface. The transporting objects were synthesized by immobilizing *Synechocystis* sp. PCC 6803 cells on amine-functionalized magnetic beads with 2.8 μm diameters by means of EDC–NHS coupling chemistry. The forces responsible for directional control of the beads loaded with microorganisms on a half-disk permalloy magnetic pattern were calculated by Maxwell 3D software under an applied field of 10 mT. These calculations suggested that the driving force experienced at the curved edge was larger than the force experienced at the flat edge, resulting in the directional translocation of beads along the curved edge.

The *Synechocystis* sp. PCC 6803 cells immobilized on the magnetic beads were directionally manipulated along a

magnetic rail track pathway and successfully trapped in a magnetic trapping station. This approach has a number of compelling features including the following: (1) It generates no heat, (2) it allows long-distance regional manipulations over a few hundred micrometers, (3) it provides directional manipulation, (4) it has the capability to trap the single microorganism, and (5) it allows programmable manipulation. Efforts are underway to use this manipulation and trapping technique to analyze the contents of individual microorganisms by integrating the technique with lab-on-a-chip systems.

References

Anandakumar S, Rani VS, Jeong JR, Kim CG, Kim KW, Rao BP (2009) Translocation of magnetic beads using patterned magnetic pathways for biosensing applications. J App Phys 105:07B312

Anandakumar S, Rani VS, Sunjong Oh, Sinha BL, Takahashi M, Kim CG (2010) Translocation of bio-functionalized magnetic beads using smart magnetophoresis. Biosensors and Bioelectron ics 26:1755

Anderson SL, Mcintosh L (1991) Light-activated heterotropic growth of the cynaobacterium synechocystis sp. strain PCC 6803: a blue-light-requiring process. J Bacteriol 173:2761

Brzeska M, Panhorst M, Kamp PB, Schotter J, Reiss G, Pühler A, Becker A, Bruckl H (2004) Detection and manipulation of biomolecules by magnetic carriers. J Biotechnol 112:25

Deng T, Whitesides GM, Radhakrishnan M, Zabow G, Prentiss M (2001) Manipulation of magnetic microbeads in suspension using micromagnetic systems fabricated with soft lithography. Appl Phys Lett 78:1775

Duffy DC, McDonald JC, Schueller OJA, Whitesides GM (1998) Combinatorial synthesis of highly selective cyclohexapeptides for separation of amino acid enantiomers by capillary electrophoresis. Anal Chem 70:4974

Elizabeth R, Geoffery SDB (2012) Dynamics of superparamagnetic microbead transport along magnetic nanotracks by magnetic domain walls. Appl Phys Lett 100:08240

Gijs MAM (2004) Magnetic bead handling on chip: New opportunities for analytical applications Microfluidics and Nanofludics 1(1):22

Gunnarsson K, Roy PE, Felton S, Pihl J, Svedlindh P, Berner S, Lidbaum H, Oscarsson S (2005) Programmable motion and separation of single magnetic particles on patterned magnetic surfaces. Adv Mater 17:1730

Hu X, Lim, B, Jung, I, Sandhu A, Kim CG (2012) Optimization of pathway pattern size for programmable biomolecules actuation (Submitted to IEEE Trans Magn)

Hunt TP, Isssadore D, Weatervelt RM (2008) Integrated circuit/microfludic chip to programmably trap and move cells and droplets with dielectrophoresis. Lab Chip 8:81

Ito A, Shinkai M, Honda H, Kobayashi T (2005) Medical application of functionalized magnetic nanoparticles. 100:1

Johansson L, Gunnarsson K, Bijelovic S, Eriksson K, Surpi A, Gothelid E, Svendlindh P, Oscarsson S (2010) A magnetic

microchip for controlled transport of attomole levels of proteins Lap Chip 10:654

Karle M, Miwa J, Czilwik G, Auwarter V, Roth G, Zengerle R, von Stetten F (2010) Continuous microfluidic DNA extraction using phase-transfer magnetophoresis. Lab Chip 10:3284

Karle M, Wohrle J, Miwa J, Paust N, Roth G, Zengerle R, von Stetten F (2011) Controlled counter-flow motion of magnetic bead chains rolling along microchannels. Microfluidics and Nanofludics 10:935

Krylov S, Dovichi N (2000) Single cell analysis capillary electrophoresis: influence of surface support properties on cell injection into the capillary. Electrophoresis 21:767

Lindstrom S, Andersson-Svahn H (2010) Overview of single-cell analyses: microdevices and applications. Lap Chip 10:3363

Liu HH, Duan XK, Che RC, Wang ZF, Duan XF (2009) In situ lorentz microscopy observation of displaced chain walls in permalloy. Mater Trans 50:1660

Pawel LU, Thomas S, Andrea A, Reanto Z (2011) Multidimensional analysis of single algal cells by integrating microscopy with mass spectrometry. Anal Chem 83:1843

Ramadan Q, Samper V, Poenar DP, Yu C (2006) An integrated microfluidic platform for magnetic microbeads separation and confinement. Biosens Bioelectron 21:1693

Safarik I, Safarikova M (2004) Magnetic techniques for the isolation and purification of proteins and peptides Biomagn Res Tech 2:7

Schubert H, Schiewer U, Tschirner E (1989) Fluorescence characteristics of cyanobacteria J Plankton Res 11:353–359

Sinha B, Anandakumar S, Sunjong O, Kim CG (2012) Micro-magnetometry for susceptibility measurement of superparamagnetic single bead. Sensors and Actuators A 182:34

Smistrup K, Torsten L-O, Hansen, MF, Tang PT (2006) Microfluidic magnetic separator using an array of soft magnetic elements. J Appl Phys 99:08P102

Varadan, KV, Chen L, Xie J (2008) Nanomedcine. Wiley, UK

Wirix-Speetjens R, Fyen W, Xu K, Boeck JD, Borghs G (2005) A force study of on-chip magnetic particle transport based on tapered conductors IEEE Trans Magn 41:4128